

Sublimate speciation at Mutnovsky volcano, Kamchatka

MICHAEL ZELENSKI^{1,*} and SVETLANA BORTNIKOVA²

¹Institute of Volcanology, Piip Boulevard 9, Petropavlovsk-Kamchatsky, 683006, Russia

²Institute of Geology, Koptyug Pr. 3, Novosibirsk 630090, Russia

Abstract: Sublimates from high-temperature (470-507°C) gases at Mutnovsky volcano in southern Kamchatka were collected in silica glass tubes. Only particles of altered rocks were found in a transparent zone above 480°C. From 480 to 120°C, Fe and Cd sulphides with or without NaCl change to Cd-Pb-Bi and Pb-As-Bi sulphosalts, Pb-As and Bi sulphohalides, Cd, Pb, Tl halides, and an amorphous As-S compound. Sublimates are especially enriched in cadmium, thallium and iodine. Two new Cd-bearing sulphosalts $Cd_4PbBi_{12}(S,Se)_{23}$ and $CdPb_4Bi_6(S,Se)_{14}$ containing respectively 9 and 4 atomic% Cd were described. Tl occurs as three different halides. Seven phases contain iodine as a major or minor component; four of them additionally contain bromine. Crystal sizes, shapes and quantity within deposition intervals vary according to nucleation conditions. Mineral assemblages in natural fumarolic incrustations partly repeat the sequence observed in silica tubes.

Key-words: sublimates, Mutnovsky volcano, volatile transport, Cd sulphosalts, Tl - I - bearing phases.

Introduction

Volcanic gases consist of major components (H_2O , CO_2 , sulphur and haloid species, N_2 , sometimes O_2), rare gases, and multiple volatile species of trace elements. Cooling of gases during discharge causes elements to precipitate as solid phases (sublimates). Phase and chemical composition of sublimates is determined by chemical and physical properties of volcanic gases they are precipitated from; therefore sublimates serve as a tool for studying volcanic gases. On the other hand, sublimates may attract attention themselves as rare phases with uncommon chemical compositions. They frequently consist of rare and scattered elements, thus sublimates research essentially broadens the scope of mineralogy.

Sublimates vary from one volcano to another, but there is a general temperature order appropriate for reducing conditions: a) oxides and Na-K halides; b) sulphides and sulphosalts; c) low-temperature halides; d) arsenic-bearing phases and native sulphur. A thermochemical approach explains the deposition sequence (Symonds *et al.*, 1987; Symonds & Reed, 1993), even though gases do not reach complete equilibrium with precipitating sublimates (Symonds, 1993). The transport of elements occurs as halide species and some other forms including sulphides, acid and native elements (Symonds *et al.*, 1987, 1992; Symonds & Reed, 1993; Taran *et al.*, 2001).

Mutnovsky volcano in Kamchatka is famous for its various and intensive hydrothermal manifestations (Vakin *et al.*, 1976; Taran *et al.*, 1992), with the highest temperatures exceeding 500°C. Previous studies at the volcano concerned geology (Selyangin, 1993), heat flow measurements (Polyak, 1966; Myravyev *et al.*, 1983), geochemistry of major gas species (Serafimova, 1966; Taran *et al.*, 1992) and mineralogy of low-temperature fumaroles (Serafimova, 1979). Volatile transport of elements and mineral parageneses of high-temperature fumarolic fields were completely unknown until recent years. To evaluate heavy metal emissions and succession of mineral precipitation from high-temperature fumarolic gases at Mutnovsky volcano, we collected gas samples and sublimates in silica glass tubes, as well natural incrustations during summer months in 2000-2002. The purpose of this work is to present the phase and chemical compositions of sublimates in silica tubes from Mutnovsky. The article also shortly describes related compositions of gases and natural incrustations.

Geological setting and current activity of Mutnovsky volcano

Mutnovsky (52.35°N, 158.27°E, 2323 m) is a stratovolcano in southern Kamchatka, 75 km south from the town of

*E-mail: ppm61@mail.ru

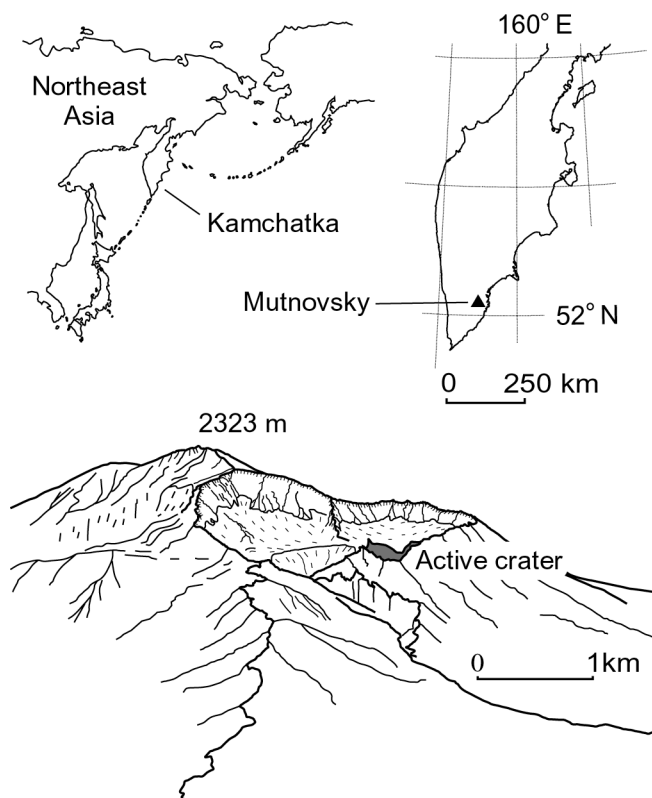


Fig. 1. Mutnovsky volcano and its geographical position. The active crater is situated on the northwestern slope 3 km from the main summit.

Petropavlovsk-Kamchatsky, 20 km from the Pacific coast. The volcano has a complex edifice (Fig. 1) and various rock compositions. High-alumina basalts and basaltic andesites predominate, but there are several small rhyodacitic domes on the northern flanks (Selyangin, 1993). Two huge old craters (1.5×2 and 1.3×1.3 km) are partly filled with ice. The active crater, an explosive crater

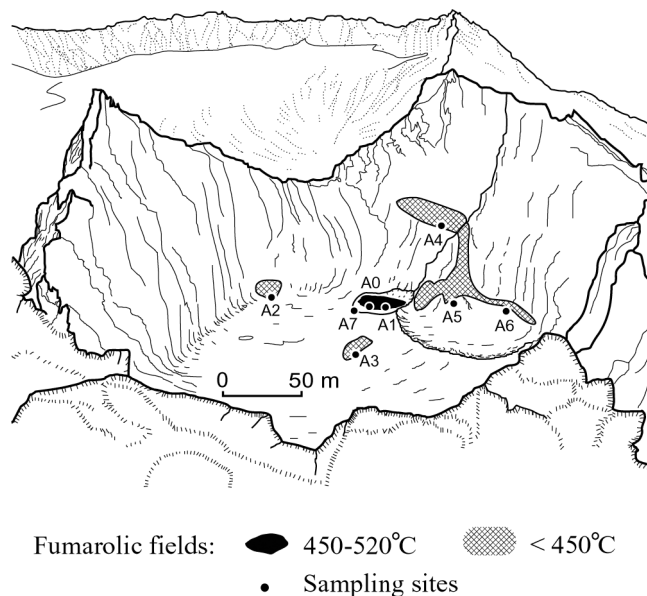


Fig. 2. Location and temperatures of fumarolic fields in the Mutnovsky active crater.

350×450 m with steep rock walls of up to 200 m and a flat bottom is situated 3 km northwest from the main summit.

Recent activity of Mutnovsky is characterized by weak phreatic and phreato-magmatic explosions, approximately one in 40 years. The last explosion occurred in March 2000 (Zelenski *et al.*, 2002); a warm lake of 250 m width was formed in a new explosive crater two months later. A variety of permanent fumaroles exist at the volcano. Three fumarolic fields with temperatures 98-262°C (in 2002) and low magmatic component (< 10 %) are situated in the lowest part of the old northeast crater. More than 80 % of volcanic gases discharge from the active crater. Fumaroles with temperatures over 400°C exist at the crater periphery (Fig. 2). The hottest fumaroles (450-524°C in 2002) are

Table 1. Major gas species (mg/kg) and isotopic composition (δD and $\delta^{18}O$, permil relative to VSMOW) for fumaroles of Mutnovsky volcano.

	A1	A2	A3	A4	A5	A6	A7	A8	A9
T, °C	507	196	309	240	410	450	383	153	281
H ₂ O	928000	938000	941000	918000	923000	914000	925000	971000	983000
CO ₂	32800	21600	33400	25900	34500	24800	38800	12300	13700
H ₂ S	5800	6300	2900	10300	5700	8800	5700	5100	1100
SO ₂	28500	29600	18600	41000	31400	46300	26000	3100	1500
HCl	3400	3750	2850	3950	3850	4600	2900	4800	80
HF	660	80	450	140	820	870	370	28	8
CO	3.60	0.0068	0.010	0.0068	0.19	0.34	0.088	0.12	0.0098
CH ₄	0.092	0.10	0.091	0.045	0.064	0.040	0.13	2.5	28
H ₂	33	0.26	0.89	0.79	5.2	13	3.5	0.93	0.55
He	0.017	0.012	0.02	0.014	0.018	0.014	0.023	0.019	0.0025
δD , ‰	-81.6	-76.5	-87.7	-69.8	-74.9	-64.0	-80.8	-84.9	-109.9
$\delta^{18}O$, ‰	-3.5	-3.2	-4.6	-0.9	-2.3	1.0	-4.1	-6.0	-11.3

Samples: A1-A7 - active crater; A8, A9 – northeast crater. Isotopic definitions for gas condensates were performed by E. Dubinina (IGEM RAS, Moscow).

concentrated on an oblique outcrop 10 × 25 m of fractured altered basalts. Gas discharges with low noise from holes and open fractures up to 10-15 cm wide. Rocks are covered with white, dark-grey and orange incrustations. Temperatures and rates of emissions here are relatively constant at least since 1984 (Taran *et al.*, 1992). In 1963-1966 temperatures above 750°C were recorded (Vakin *et al.*, 1966).

Main component of high-temperature fumarolic gases is water vapour (Table 1). Gases are characterized by high content of sulphur species, and high HF/HCl ratio. Concentrations of minor elements in condensates from Mutnovsky are listed in Table 2. δD - $\delta^{18}O$ analyses have shown 31-58 % of magmatic component (Zelenski, 2003).

Sampling and analytical methods

Sublimates were collected in silica glass tubes with a method used for the first time by Le Guern & Bernard (1982). Tubes 0.5-1 m long and 10-20 mm inner diameter were inserted into fumarolic vents with temperatures from 470 to 507°C. Gases passed through tubes, which are cooled with ambient airflow. To obtain the full range (507-120°C) of temperature inside a single tube, the hot ends were flattened to slow down gas flux. Temperatures were measured by a chromel-alumel thermocouple along the inside walls of the tubes and across the outlet. Measurements were done immediately after inserting the tubes into a vent, and before removing them; no significant difference was noticed between two measurements. Regardless of measurement precision, acquired curve may represent only a crude approximation of the temperature distribution along the tube length. The real temperature curve is subject to change. It depends on the weather conditions, as the tubes are cooled by the ambient airflow (Tkachenko *et al.*, 1999). The deposited sublimates also depress heat transfer through the tube walls. Temporary thermal crises even cause melting of various solid species *e.g.* thallium iodide and sulphur. The gas flux has also radial temperature distribution with hot axial and cool peripheral parts that leads to noticeable perpendicular zoning. Therefore, some relatively high-temperature phases were deposited in close proximity to the "coldest" ones.

Rates of sublimates growth at Mutnovsky volcano are small as a result of relatively low temperatures and low element concentrations in gases. Accordingly to get good samples, tubes remained in the vents for 60-120 days. Nine tubes with sublimates were collected.

In the laboratory the tubes were broken into pieces 2-5 cm long. The tubes were split instead of cut with a diamond saw, to avoid contamination with silica mud. First of all the samples were examined through an optical binocular microscope with magnifications up to 200 \times . After preliminary visual inspection, individual phases were picked up and analysed with X-ray diffraction. For abundant phases (*e.g.* sulphosalts) investigations were carried out by means of conventional X-ray diffractometer (FeK α radiation). Many of the phases, however, were found as scattered small crystals or thin coating; to investigate these a Debye-

Sherrer camera (FeK α radiation) was used. Morphology and chemical composition of the sublimates were studied by SEM with an EDS device. Sulphosalts were analysed by means of an electron microprobe with wavelength-dispersive spectrometers because quantitative analysis of Pb-Bi sulphosalts with energy dispersive spectroscopy is not optimal due to overlapping peaks. Some phases (especially halogen-bearing) appeared to be unstable under the electron beam, or to form tiny crystals; hence sums of analyses were significantly less than 97.5 %. Such analyses were considered as semiquantitative. Another problem was wide isomorphism (*e.g.* I-Cl-Br, Bi-As-Al), leading to variable analyses for a single phase. Therefore the chemical compo-

Table 2. Trace elements in condensate samples from the hottest fumaroles of Mutnovsky volcano (mg/kg).

Element	A0	A1	A5	A6
Li	0.002	0.002	0.005	0.003
B	27	26	18	25
Na	18	2.3	4.6	8
Mg	0.28	0.45	0.55	0.28
Al	4.8	2.2	1.6	2.1
Si	33	29	69	112
K	2.2	1.5	1.6	1.6
Ca	2.8	1.8	1.9	3.1
Ti	0.087	0.078	0.093	0.11
V	0.019	0.017	0.017	0.015
Cr	0.02	0.015	0.009	
Mn	0.017	0.013	0.007	0.009
Fe	2.1	1.1	0.61	0.61
Ni	0.019	0.016	0.004	0.01
Cu	0.008	0.026	0.003	0.008
Zn	0.048	0.16	0.06	0.07
Ga	0.002	0.002	0.001	0.001
As	3.8	4.7	6.9	8.6
Se	0.29	0.11	0.32	0.5
Br	3.8	3.7	4.0	6.0
Rb	0.001	0.003	0.003	0.003
Sr	0.014	0.026	0.006	0.011
Zr	0.025	0.055	0.056	0.092
Nb	0.002	0.002	0.001	0.015
Mo	0.005	0.005	0.001	0.005
Ag	0.001	0.006	0.001	0.001
Cd	0.032	0.025	0.007	0.011
Sn	0.014	0.017	0.005	0.008
Sb	0.012	0.019	0.013	0.03
Te	0.12	0.145	0.253	0.349
I	0.35	1.1	1.1	1.7
Ba	0.085	0.017	0.008	0.02
Hf	0.0007	0.0009	0.0007	0.0015
W	0.001	0.006	0.003	
Hg	0.047	0.16	0.23	0.19
Tl	0.11	0.098	0.031	0.036
Pb	0.14	0.13	0.025	0.04
Bi	0.067	0.063	0.033	0.065
Th	0.0002	0.0006	0.0001	0.0002

Samples: A0, A1, A5, A6 - active crater (480, 507, 410, 450°C respectively). Elements that form their own species in sublimates are given in bold. Be, Sc, Co, Ge, Y, Ru, Rh, Pd, Cs, Ta, Os, Ir, Pt, Au, U, La and all lanthanides are not included because more than 50 % of the data were below the detection limit.

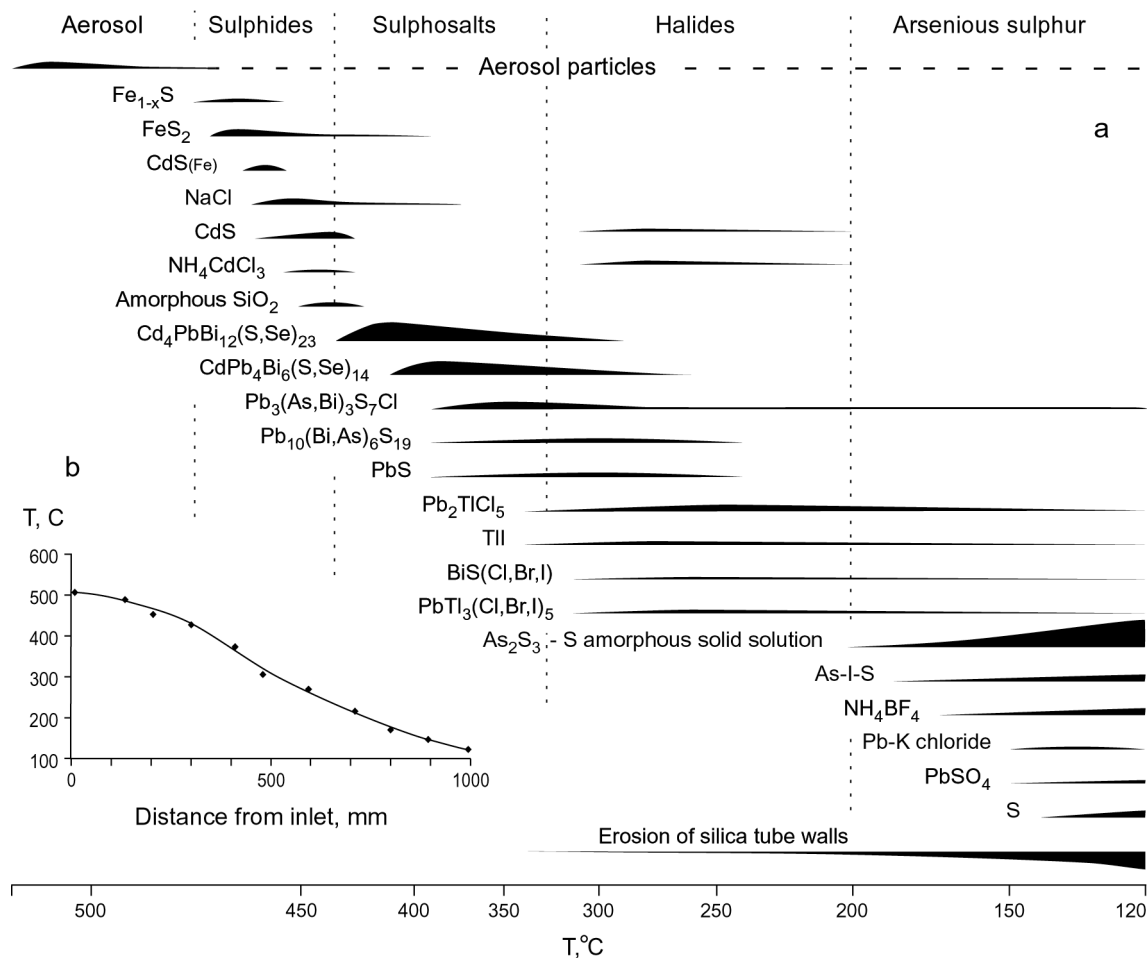


Fig. 3. Observed deposition sequence of sublimates in the silica tubes as a function of temperature (a) and temperature distribution along the tube (b). The plot represents the average for all collected tubes.

sition of several phases remains uncertain. At least two XRD and two quantitative (or semiquantitative) analyses were obtained for each phase. For known phases, their

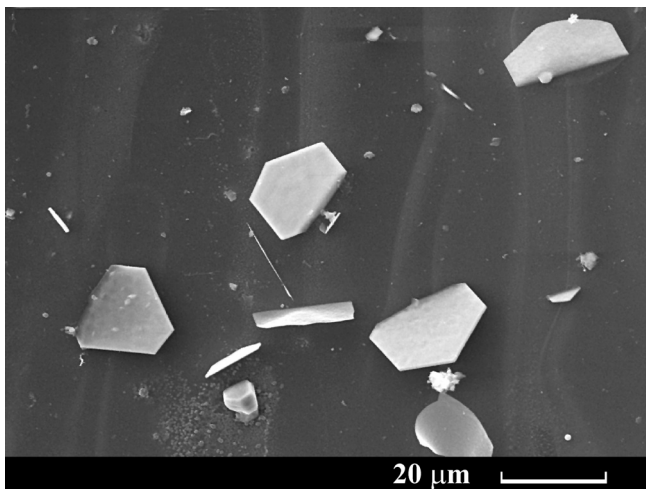


Fig. 4. Hexagonal pyrrhotite platelets on the glass surface (BSD image).

theoretical formulae are presented. If the phase proved to be unknown, its formula was calculated using available analyses. Reliability of such calculated formulae depends on the number of analyses and their dispersion. Large and widespread crystals of sulfosalts were analysed dozens of times, but some rare phases (*e.g.* bismuth sulphohalide) have only a few highly variable analyses.

Sublimates from one representative tube were used to determine bulk elemental composition. Mineral precipitates from each 10 cm section were entirely scraped off and weighed. Then precipitates were analysed by ICP-MS and ICP-AES techniques. Concentrations in such analyses were normalized to total weight of precipitates in each 10 cm section.

All concentrations of elements, if not noted otherwise, are given in atomic%.

Sublimate mineralogy

Twenty-one phases have been identified in the tubes. There is a clear temperature-dependent succession of the deposited solid phases (Fig. 3). From 480 to 120°C, simple Fe and Cd sulphides with or without NaCl are followed by

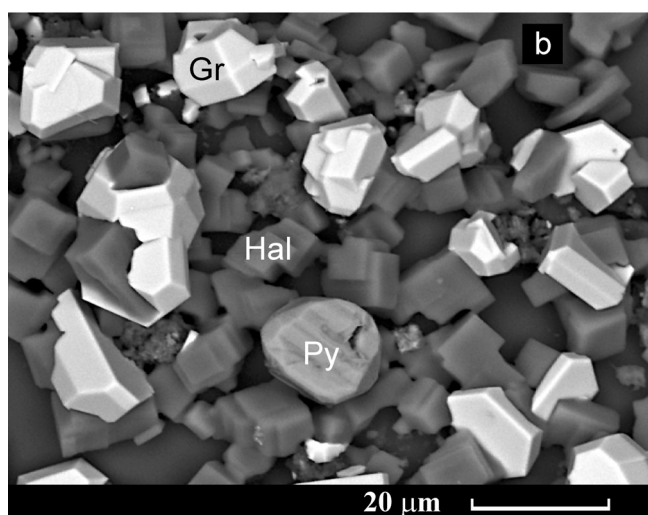
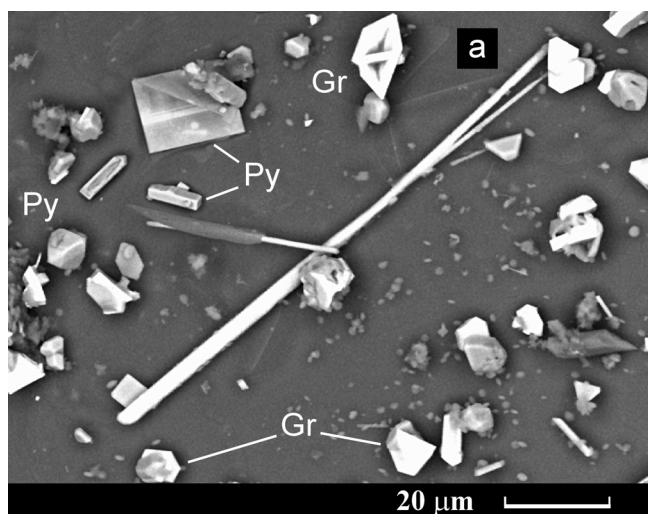


Fig. 5. Simultaneous precipitation of sulphides and halides in the high-temperature zone. Needle-shaped crystals of NH_4CdCl_3 on the glass surface (a). Truncated hexagonal pyramids of greenockite scattered on glass (a) or distributed among cubic halite crystals (b). Pyrite forms octahedral, elongated or bladed crystals (a). Both BSD images. Hal – halite, Gr – greenockite, Py – pyrite.

Cd-Pb-Bi and Pb-As-Bi sulphosalts, Pb-As and Bi sulphohalides, and Cd, Pb, Tl halides (Fig. 3). The lowest-temperature phases are As-S and As-S-I compounds. Deposition sequences differ slightly from one tube to another; the most important distinction is the absence of NaCl in several tubes. Each phase precipitates in its own temperature interval and has more or less diffuse limits of occurrence; one exception is a rather narrow overlapping zone between greenockite and sulphosalts. Generally, crystals are large and well shaped at the first, high-temperature appearance of the phase, and change into numerous tiny subhedral crystals at the low-temperature occurrence. On average, crystal sizes are 5-10 μm ; only one sulphosalt forms elongated flat crystals up to 250 μm . However, the predominating phase in the sublimate (up to 90 %) is non-crystalline, X-ray amorphous arsenious sulphur.

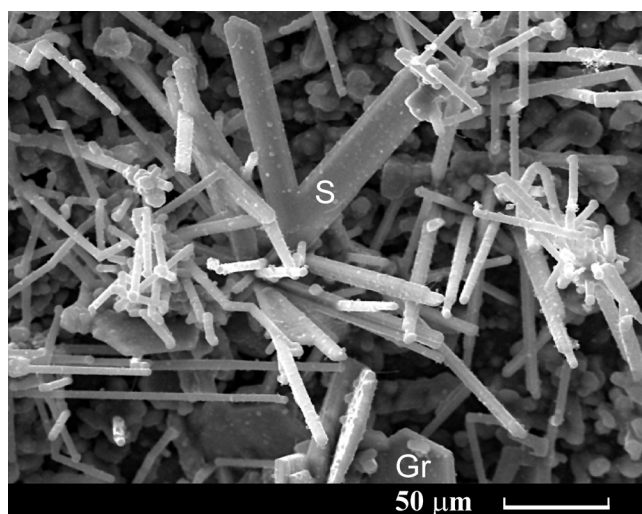


Fig. 6. X-ray amorphous silica needles (white) together with sulphosalt (S) and greenockite (Gr). SE image.

No precipitates except aerosol particles were detected above 480°C in a transparent zone at the hot ends of the tubes. These particles, 0.1-0.2 mm size or less, are mainly small aggregates and crystal fragments of rock-forming minerals (plagioclase, pyroxene) and gas-rock interactions products, as aluminium hydroxide, anhydrite, hematite, magnetite, and cristobalite. Small amounts of aerosol particles are scattered along the whole length of the tubes.

The first sublimate crystals, hexagonal platelets of pyrrhotite $\text{Fe}_{(1-x)}\text{S}$ (Fig. 4), appear at 480°C. The next two phases are pyrite FeS_2 and greenockite CdS (Fig. 5a, 5b). Two distinct kinds of greenockite were found: a high-temperature greenockite containing ~ 8 % Fe with subhedral ruby-coloured crystals, and “normal” greenockite, which contains 2-2.5 % Fe and forms euhedral hexagonal pyramidal brown crystals. Apart from other halides, thin colourless needles of ammonium-cadmium chloride NH_4CdCl_3 (Fig. 5a) and halite (NaCl) occur together with sulphides. Halite displays cubic crystals at the highest temperatures of occurrence (Fig. 5b). At lower temperatures halite exhibits extraordinary anisotropic habits – long, flat or square-section needles. Similar anisotropy of some sublimate phases was noticed earlier (Symonds, 1993) and has no satisfactory explanation yet. One more example of anisotropy is X-ray amorphous silica, which forms colourless whiskers in a narrow stripe following just after the halite-greenockite zone (Fig. 6). Small “heads” on the tips of each needle are visible; they probably indicate growths from liquid droplets. No detectable admixture of any element except Si and O was analysed in the phase. Halite, NH_4CdCl_3 and amorphous silica are present only in four tubes.

Sulphosalts are the most widespread crystalline phases among sublimate; four kinds of them were determined. The first according to temperature sequence, a sulphosalt with idealized formula $\text{Cd}_4\text{PbBi}_{12}(\text{S,Se})_{23}$ forms relatively large crystals (Fig. 7a) at the beginning of deposition (440°C) and dendrites (Fig. 7b) at lower temperatures.

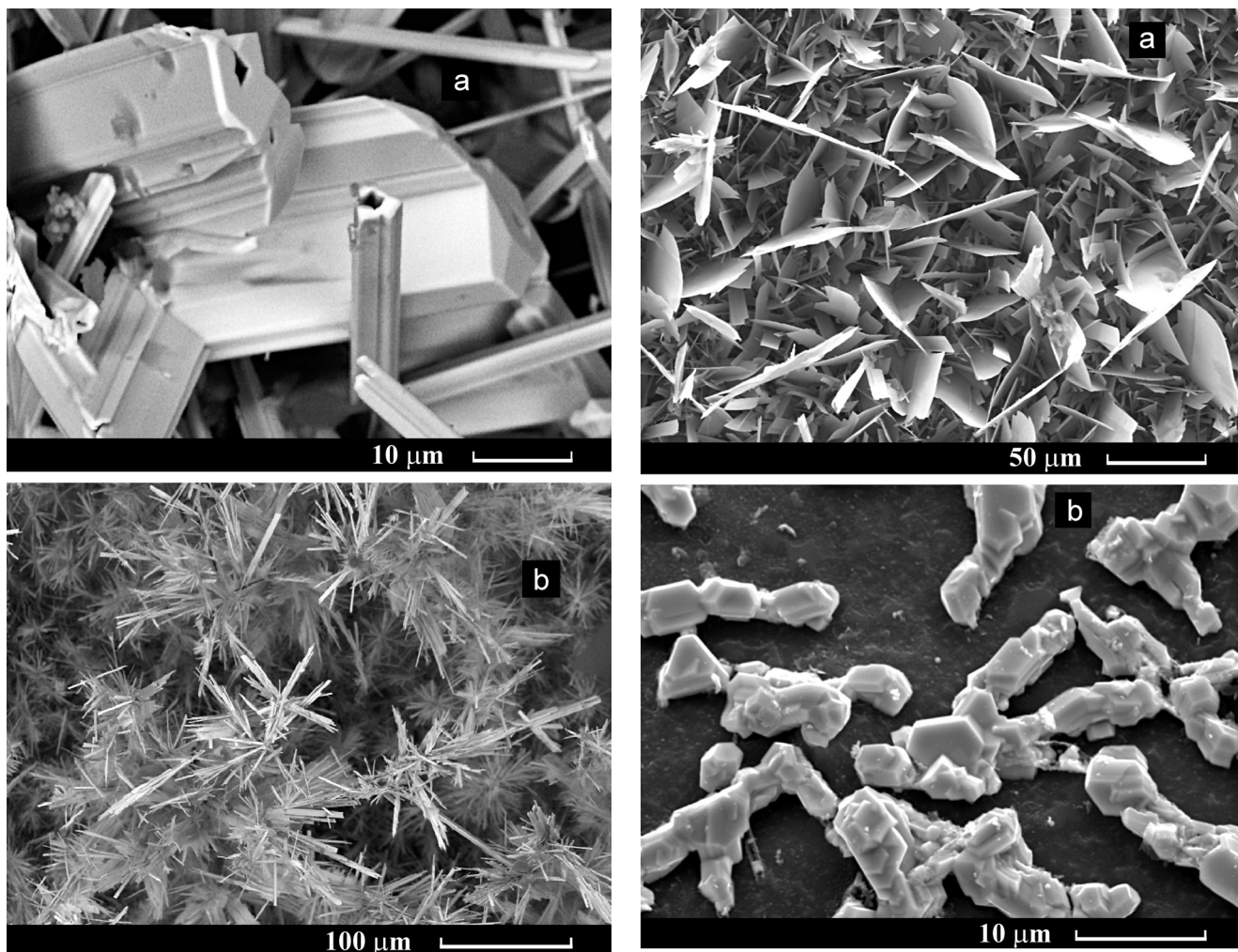


Fig. 7. Large euhedral crystals of the Cd-bearing sulphosalt $\text{Cd}_4\text{PbBi}_{12}(\text{S,Se})_{23}$ (a) and dendrites of acicular crystals (b) at high and low temperatures of deposition. Crystals usually show hatching on account of polysynthetic twinning; a tubular shape is frequent, too. Both SE images.

Phase contains 9 % Cd and ~ 3 % Se. Sulphosalt $\text{CdPb}_4\text{Bi}_6(\text{S,Se})_{14}$ has leaf-like shape of crystals (Fig. 8a) and X-ray diffraction pattern identical to cannizzarite (Mosgova *et al.*, 1985, 1998), but contains 4 % Cd. Both Cd-bearing sulphosalts are black with metallic lustre; the thinnest leaves of the cannizzarite-like sulphosalt are faintly translucent in brown. Kirkiite $\text{Pb}_{10}(\text{Bi,As})_6\text{S}_{19}$ was determined on the basis of chemical composition, X-ray pattern and distinctive tin-white pseudo-hexagonal short-prismatic crystals (Borodaev *et al.*, 1998; Fig. 8b). Halogen-bearing sulphosalt $\text{Pb}_3(\text{As,Bi})_3\text{S}_7\text{Cl}$ occurs as radiant acicular aggregates (Fig. 8c) and dendrites from approximately 380°C until the outlet. Dark-grey needles of the phase turn pink-brown when they become extremely thin. Small amounts of galena PbS , as a thin mixture with small kirkiite crystals were also discovered with XRD and EDS methods.

Different halides and sulphohalides of Cd, Tl, Pb and Bi begin to precipitate at temperatures less than 330-340°C.

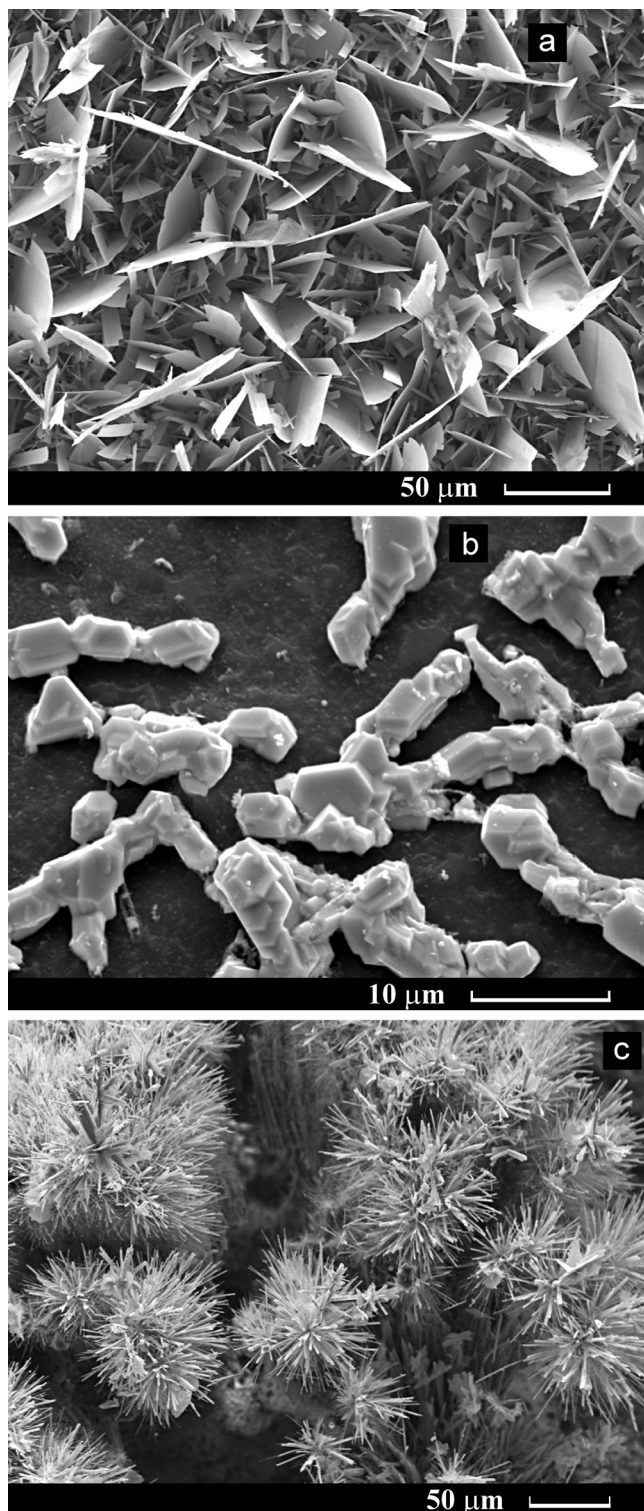


Fig. 8. Three chemically and morphologically different sulphosalts. Leaves of cannizzarite-like $\text{CdPb}_4\text{Bi}_6(\text{S,Se})_{14}$ (a). Pseudo-hexagonal crystals of kirkiite $\text{Pb}_{10}(\text{Bi,As})_6\text{S}_{19}$ with benched surface (b). Radiant acicular aggregates of Cl-bearing sulphosalt $\text{Pb}_3(\text{As,Bi})_3\text{S}_7\text{Cl}$ (c). All SE images.

Pb_2TlCl_5 is the most common halide in the zone. It occurs as isometric (Fig. 9) or elongated prismatic light-brown

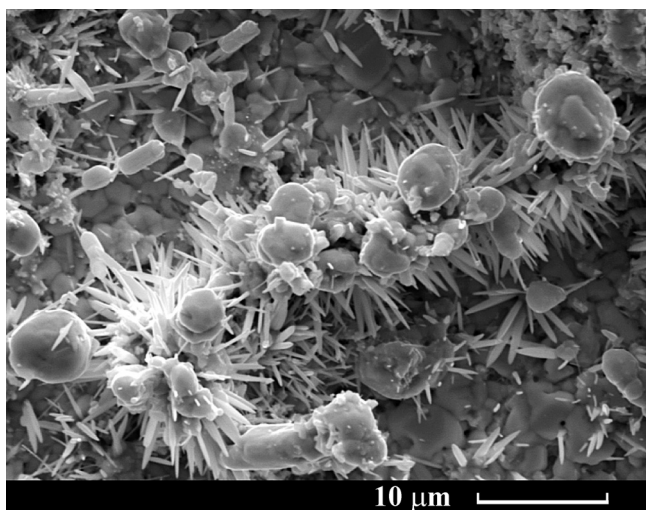


Fig. 9. Spear-shaped crystals of $\text{BiS}(\text{Cl},\text{Br},\text{I})$ and round subhedral crystals of Pb_2TlCl_5 on the surface of solid As-S compound (SE image).

crystals. X-ray diffraction pattern of Pb_2TlCl_5 almost coincides with that of Pb_2KCl_5 (27-1364 JCPDS), so these substances must be isostructural. At the same time, small acicular aggregates of undetermined Pb-K chloride were detected here only by SEM-EDS. Ammonium-cadmium chloride NH_4CdCl_3 appears once again simultaneously with minor amounts of CdS. Several iodine-bearing phases are present in the zone. The most conspicuous are euhedral, cubic or cubic octahedron, orange crystals of thallium iodide TlI , often with slightly fused facets (Fig. 10a). The complex halide $\text{PbTl}_3(\text{Cl},\text{Br},\text{I})_5$ has Cl:Br:I ratio about 1:0.2:1; it precipitates as a thin ivory coating on the glass surface. In spite of their small size ($< 3 \mu\text{m}$), crystals of the phase have clear visible octahedron and rhombic-dodecahedron habits (Fig. 10b). Bismuth sulphohalide $\text{BiS}(\text{Cl},\text{Br},\text{I})$ contains 4-10 % Cl, 4-7 % Br and 22-24 % I; As and Al partly substitute for Bi. It forms peculiar spear-shape crystals, usually in aggregates together with Pb_2TlCl_5 (Fig. 9).

A zone of X-ray amorphous arsenious sulphur follows after halides. Arsenious sulphur is present in two morphological forms: thin, yellow-orange, hollow fibres (Fig. 11a) and solid drops or a layer of arsenious sulphur compound on the glass surface. Apparently such compound forms as a result of fusion of fibres when the temperature increases. When the melt solidifies again, new fibres grow on its surface (Fig. 12a). The laboratory experiment have shown melting point of As-S fibres at 205-210°C. Both fibres and solid drops contain 24-30 % As, 0.9-1.9 % Se, 0.3-0.6 % Te, the rest is sulphur. We consider it as a non-stoichiometric As_2S_3 -S solid solution forming directly from the gas. Neither fibres nor solid drops have a X-ray pattern. One more iodine-bearing phase consisting of As, S and I, precipitates together with arsenious sulphur. It has small (pseudo?)hexagonal prismatic crystals, transparent with cherry colour, usually located on the ends of fibres (Fig. 11a). Successive cycles of fibre growth, fusion and

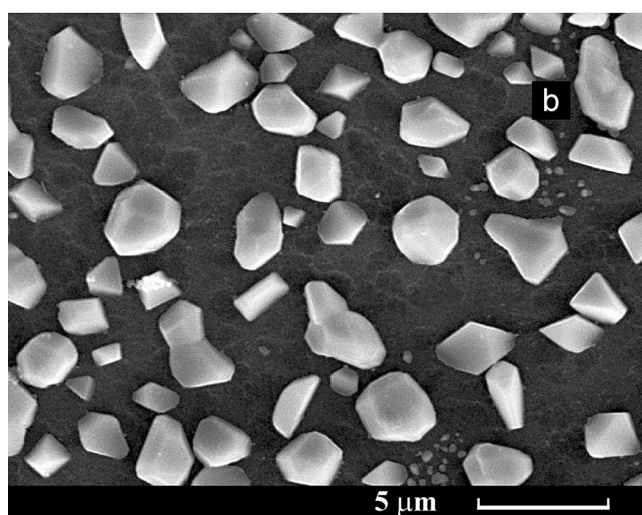
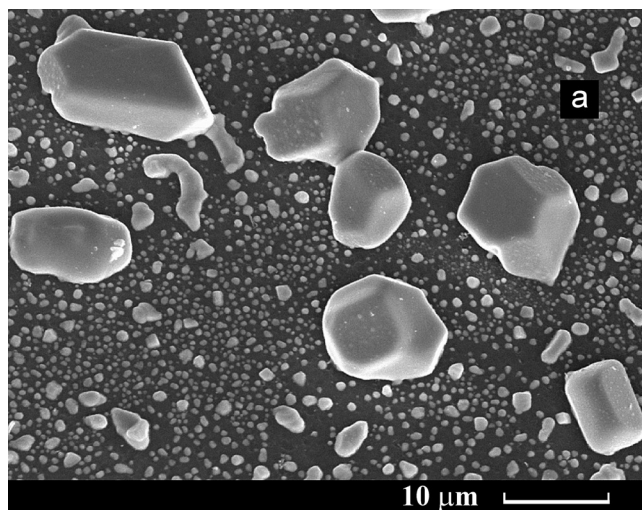


Fig. 10. Thallium iodide TlI forms cubic and cuboctahedron crystals with fused facets (a, SE image). Complex halide $\text{PbTl}_3(\text{Cl},\text{Br},\text{I})_5$ generates fine cubic, octahedron and rhombic-dodecahedron crystals (b, BSD image).

melt solidification form drops of arsenious sulphur compound with zones enriched in iodine (Fig. 11b).

Ammonium tetrafluoroborate (barberite) NH_4BF_4 deposits below 180°C together with arsenious sulphur. It occurs both as euhedral (Fig. 12) and anhedral crystals and aggregates, some of them evidently crystallized from water drops. In addition, combined aggregates of halides $\text{BiS}(\text{Cl},\text{Br},\text{I})$, Pb_2TlCl_5 (Fig. 9) and chlorine-bearing sulphosalt $\text{Pb}_3(\text{As},\text{Bi})_3\text{S}_7\text{Cl}$ grow directly on the surface of the arsenious sulphur compound. Pure native orthorhombic sulphur (with minor concentrations of As and Se) crystallizes separately from amorphous arsenious sulphur. Small anhedral crystals of anglesite PbSO_4 dispersed in an arsenious sulphur compound occur at the lowest temperature.

Along with sublimate precipitation, erosion of the silica glass walls takes place. The first signs of erosion become noticeable at 340°C as a light opaque coating on the smooth glass surface. The magnitude of erosion rapidly increases where the temperature was lower (Fig. 3).

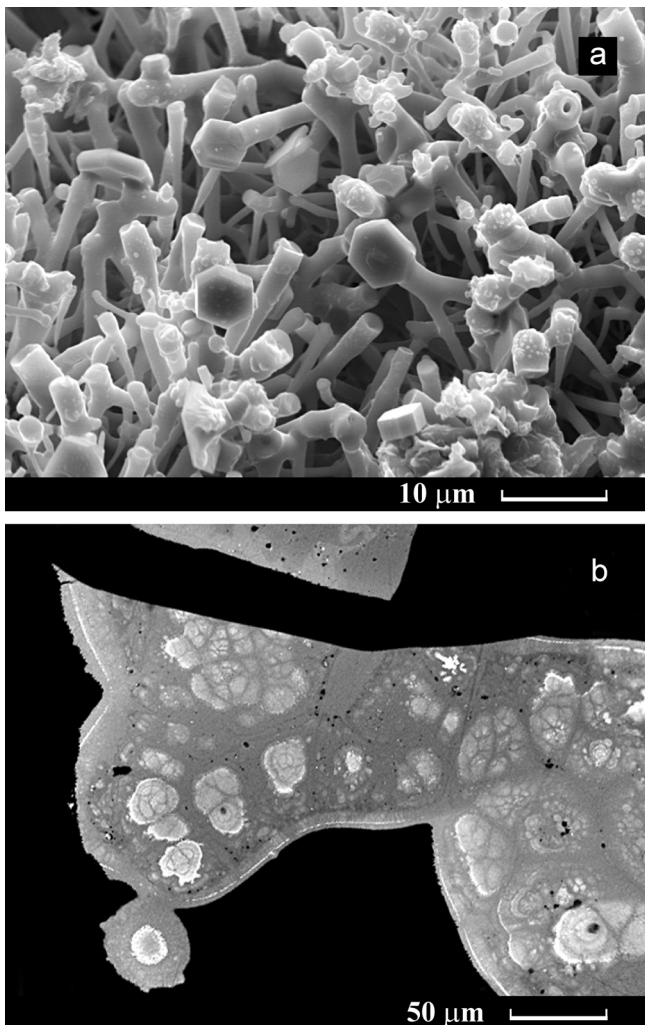


Fig. 11. Hollow fibres of X-ray amorphous arsenious sulphur with hexagonal (or pseudo-hexagonal) prismatic crystals of As-S-I species on the ends of such fibres (a, SE image). Solid drops of As-S compound with zones enriched in iodine (b, BSD image).

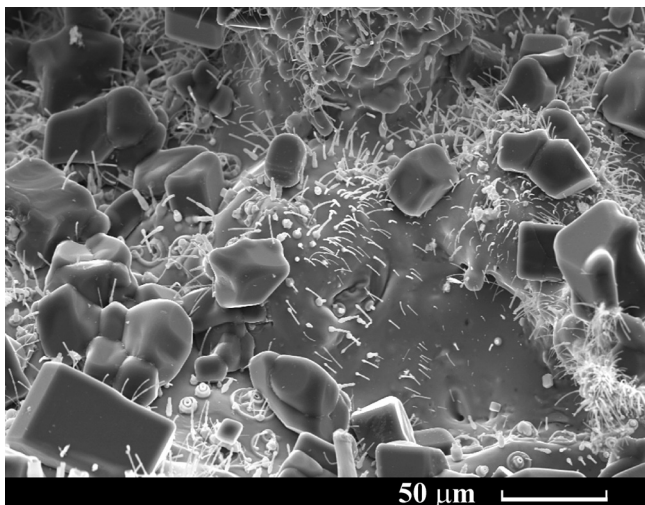


Fig. 12. As-S compound serves as a substrate for deposition of low-temperature phases, e.g. barberite NH_4BF_4 (euhedral crystals). New fibres of arsenious sulphur grow as well.

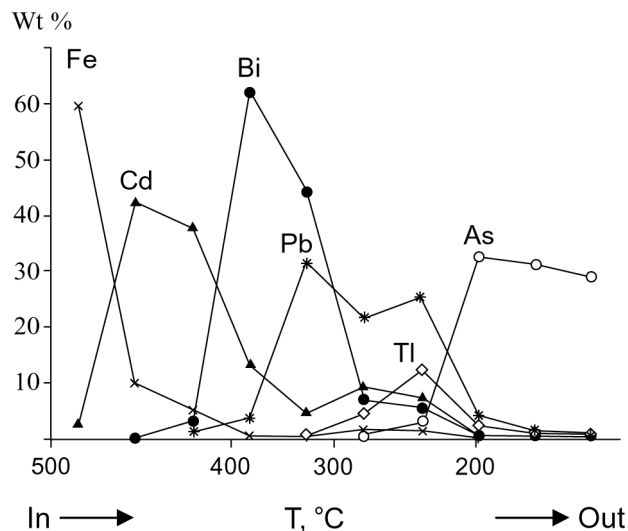


Fig. 13. Concentrations of main elements Fe, Cd, Bi, Pb, Tl, As along the tube length; only for one “representative” tube. Concentrations are given in weight% and normalized to the total weight of sublimates in each 10 cm section; the vertical axis is linear.

Cavities of up to 500 μm occur where temperatures are slightly above 100°C.

Element distribution along silica tubes

The most abundant cation-forming elements form clear visible temperature-dependent deposition sequence: Fe-Cd-Bi-Pb-(Pb+Tl)-As (Fig. 13), which is correlated with related solid phases (Fig. 3). Fe, Cd and especially Pb have the first high-temperature deposition maximum in sulphide zone and the second low-temperature deposition maximum in halide zone. Bi has one maximum in sulphide zone, and Tl has one maximum connected with different halides. Arsenic occurs in kirkiite, but its main deposition takes place in the form of amorphous arsenious sulphur. It is the second most abundant element in precipitates after sulphur; total arsenic content exceeds 27 wt.%. Arsenic abundance in sublimates is in agreement with its high concentration in gases (6-8 ppm). In contrast to arsenic, boron precipitates only in small quantities at the lowest temperatures as NH_4BF_4 though it is the most abundant (18-27 ppm) microelement in gases.

Se and Te have a different behaviour during precipitation. Both Se and Te associate with arsenious sulphur, but only Se is present in two sulphosalts. The total ratio S:Se:Te for sublimates is 30:1:1 versus 100,000:1:1 for fumarolic gases.

Fe has two solid species (pyrrhotite and pyrite), at the same time Fe appears as a minor constituent of greenockite (1.5-8 %) and sulphosalts (0.4-0.5 %). Up to 2 % Al substitutes for Bi in sulphohalide $\text{BiS}(\text{Cl}, \text{Br}, \text{I})$.

Refractory elements such as Mg, Ca, Sr, Ba, Al, Ti and Zr show almost identical distribution along tubes length (Fig. 14) with high inter-correlations (0.90-0.98). This

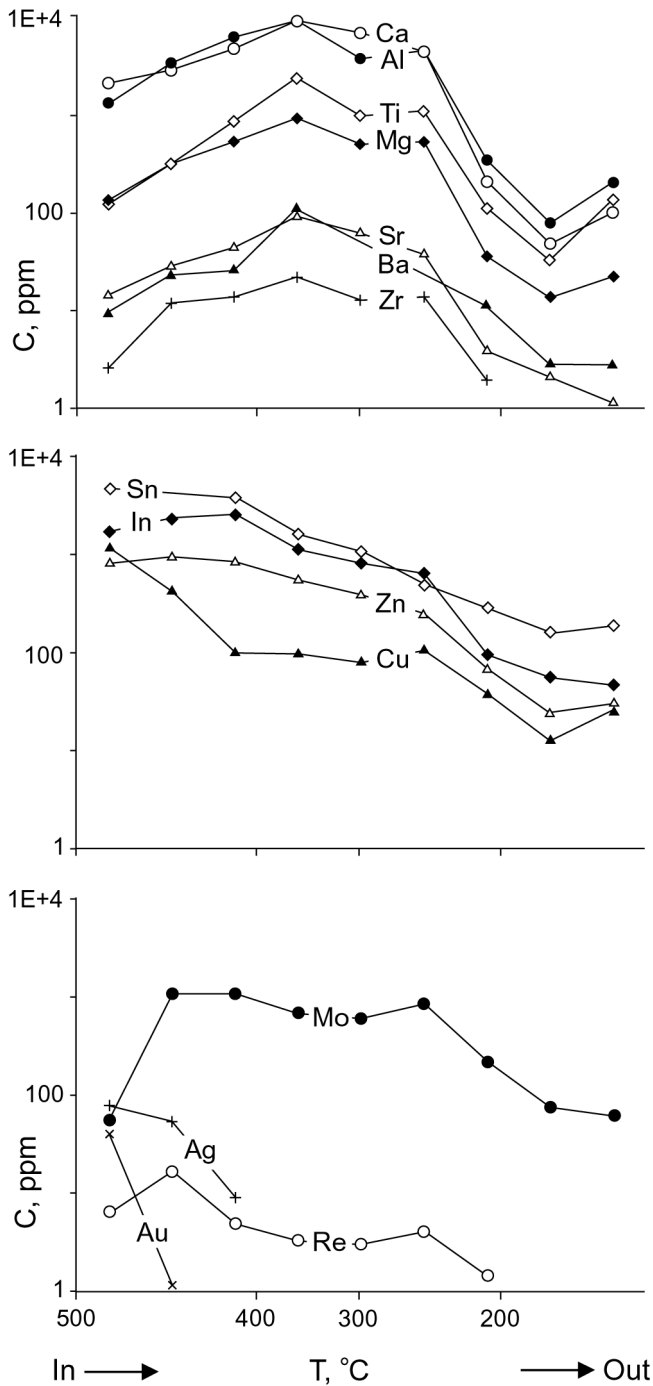


Fig. 14. Concentrations of refractory elements Mg, Ca, Sr, Ba, Al, Ti, and Zr; minor elements Sn, In, Zn, Cu, Mo, Re, Ag and Au along the tube length; only for one "representative" tube. Concentrations are given in ppm and normalized to the total weight of sublimates in each 10 cm section; the vertical axis is logarithmic.

allows for the hypothesis that refractory elements are transported mainly with the same aerosol particles.

Some minor elements are enriched at the hot ends of the tubes (Fig. 14). ICP-MS and ICP-AES analyses have shown up to 0.5 % Sn, 0.25 % In, 0.1 % Cu, Zn, Mo (all wt.%). Low concentrations of precious metals were also

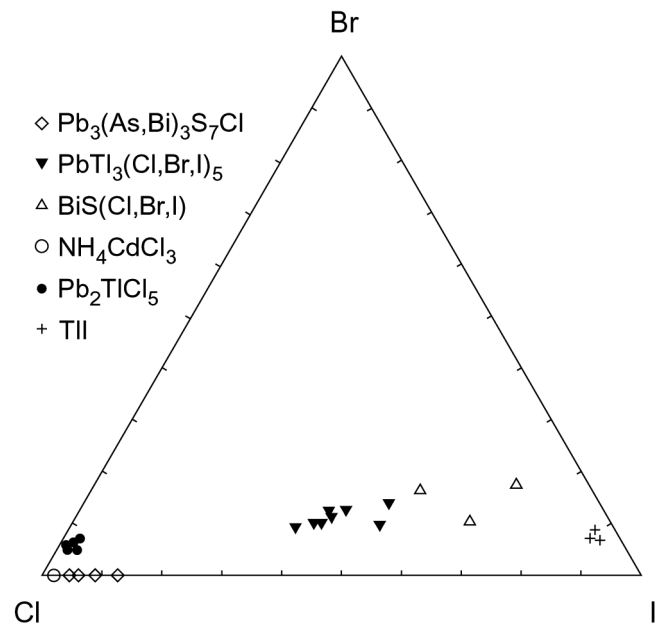


Fig. 15. Relative amounts of Cl, Br and I in halogen-bearing phases in sublimates. Note that five analyses of NH_4CdCl_3 lie at the same point.

determined here: Ag, Au (50-75 ppm), Re (6-17 ppm) and Pt (1 ppm). A similar distribution of Mo and Re suggests these elements occur in the same undetected phase. Other minor elements may exist either as isomorphous admixture in main phases or form minute crystals that are difficult to detect.

Sublimates are depleted in K compared to Na. Up to 2 % Na and K substitute for NH_4 in NH_4CdCl_3 . K in halite and both Na and K in ammonium tetrafluoroborate are below detection limit for EDS. In contrast to Mutnovsky, potassium phases are common in volcanic conditions.

Halides of heavy metals (Cd, Tl, Pb, Bi) contain Cl, Br and I in different ratios (Fig. 15). From 4 to 7 % Br was measured in Pb_2TiCl_5 , TlI, $\text{PbTi}_3(\text{Cl,Br,I})_5$ and $\text{BiS}(\text{Cl,Br,I})$. The last phase has Cl:I ratio equal 1:3 therefore it may be considered as bismuth sulphoiodide. Sulphosalt $\text{Pb}_3(\text{As,Bi})_3\text{S}_7\text{Cl}$ contains ~ 7 % Cl and 0.4-1.4 % I. Points scattering on the ternary plot (Fig. 15) are very likely a result of analytical errors. Phases with large crystals have minimal dispersion whereas tiny crystals produce significant variations. The total Cl:Br:I ratio for sublimates as a whole is approximately 10:0.1:1 compared to 3000:3:1 for fumarolic gases.

Discussion

Silica tubes, introduced in fumarolic vents, should be considered rather as a sophisticated method for study of volcanic gases than an independent objective for investigation. For example, condensates of volcanic gases are usually contaminated with particles from conduit walls that make the interpretation difficult (Symonds *et al.*, 1992;

Taran *et al.*, 1995). The degree of contamination is commonly unknown, but becomes especially noteworthy for low temperature gases. The standard approach to determine the possible source of trace elements in condensates is calculation of enrichment factors (Zoller *et al.*, 1983; Symonds *et al.*, 1987, *etc*). Elements with low enrichment factors are likely derived from aerosol particles. The sublimates in silica tubes offer an alternative way to estimate trace element concentrations. A certain trace element is obviously present in the gas phase only if it forms its own phase in sublimates, or is at least appreciably enriched in other sublimate phases. Exceptions are given for trace elements with high volatility even at low temperatures (B, Hg). From the present data at Mutnovsky we can conclude that Na, K, Fe, Cd, Tl, Pb, Bi, As, Se and Te are indeed present in gases although the true amount of each element remains to be discussed. On the contrary, Cu and Zn were found among sublimates only as minor enrichments. Therefore, moderate concentrations of Cu and Zn in condensates (Table 2) may most likely indicate aerosol contamination rather than true volatile transport.

A thermodynamic model is commonly used to study the volatile transport of elements. Such models are based on an assumption that thermochemical data are of sufficient quality and quantity (Symonds *et al.*, 1987). However, for some trace elements (As, Cd, Tl, Pb, Bi) only several simple species are available now. The sequence of solids observed in silica tubes allows us to estimate volatile speciation of these elements that can be used to support the thermodynamic approach. This sequence includes simple binary compounds as well as complex ones with several cations and anions (Fig. 3). Two different hypotheses can be examined: i) multicomponent gas containing both simple and complex gaseous species, with simple gaseous species providing simple solid species, and complex gaseous species condensates forming relatively complex solid compounds; ii) gas contains simple species that may form simple or complex solids depending on conditions.

In our tubes, simple cadmium sulphide CdS changes to sulphosalts, for which compositions can be re-written as $4\text{CdS}\cdot\text{PbS}\cdot 6\text{Bi}_2\text{S}_3$, $\text{CdS}\cdot 4\text{PbS}\cdot 3\text{Bi}_2\text{S}_3$, $6^{2/3}\text{PbS}\cdot\text{Bi}_2\text{S}_3\cdot\text{As}_2\text{S}_3$, and $2\text{PbS}\cdot\text{Bi}_2\text{S}_3\cdot\text{As}_2\text{S}_3$. Halides appear after sulphosalts with formulae $\text{NH}_4\text{Cl}\cdot\text{CdCl}_2$, $2\text{PbCl}_2\cdot\text{TlCl}$ and $\text{PbCl}_2\cdot 3\text{TlCl}$, and then $\text{As}_2\text{S}_3\cdot\text{S}$. It can be seen that all complex sulphides and halides are formed from binary compounds, "taken" in different ratios. This is evidence in favour of the hypothesis that As, Cd, Tl, Pb and Bi are transported mainly in form of simple species. Therefore, for these elements, even models with limited number of species can provide satisfactory results. Our own thermodynamic calculations (Zelenski, 2003) as well as many earlier works (Bernard & Le Guern, 1986; Symonds *et al.*, 1987, 1992; Churakov *et al.*, 2000) have shown that transport occurs as halides and also as sulphides or native elements, especially at high temperature.

Another use of the silica tubes method is to study natural mineral assemblages in fumarolic incrustations. It is much easier to find tiny, scarcely detectable crystals in tubes with smooth glass walls than on crumbly altered rocks. It is also simpler to determine in tubes some phys-

ical and chemical conditions *e.g.* temperature interval of formation for certain phases; similar measurements on the surface of rocks are often difficult or impossible.

There is an approximate correspondence between sublimates collected in the silica glass tubes, and natural ones at Mutnovsky volcano. Phases with deposition temperature from 500 to 350°C (simple sulphides, NaCl, two Cd-bearing sulphosalts and Cl-bearing sulphosalt) occur both in the tubes and among natural incrustations. Phases with deposition temperature lower than 350°C such as kirkiite, galena and halides were not found in natural conditions, with the exception of rare $\text{PbTl}_3(\text{Cl},\text{Br},\text{I})_5$. We account for this by a lack of suitable deposition conditions: the combination of appropriate temperatures and low oxygen fugacity is realized only in some thin subsurface fractures. On the other hand, natural Na_2SO_4 , bismuth oxysulphate $\text{Bi}_2\text{O}(\text{SO}_4)_2$, bismoclite BiOCl and anglesite PbSO_4 appear on the surface of rocks under oxidizing conditions.

Similarly to sublimates studied on Vulcano (Garavelli *et al.*, 1997; Cheynet *et al.*, 2000), Merapi (Symonds *et al.*, 1987; Symonds, 1993), Momotombo (Quisefit *et al.*, 1989) and St. Helens (Bernard & Le Guern, 1986) sulphosalts contain lead, bismuth and arsenic; unlike other volcanoes, two sulphosalts also contain 9 and 4 % of cadmium. The chlorine-bearing sulphosalt $\text{Pb}_3(\text{As},\text{Bi})_3\text{S}_7\text{Cl}$ theoretically includes 11.6 % Cl and may be considered as a phase intermediate between sulphosalts and sulphohalides. It occurs not only in the silica tubes but also as natural incrustations, together with two Cd-bearing sulphosalts. Moreover, another As-Pb sulphohalide found on the ground contains approximately 15 % S and 15 % (Cl+Br+I). Significant amounts of natural halogen-bearing sulphosalts demonstrate their stability. Earlier Garavelli *et al.* (1997) considered chloro-sulphides as metastable phases on account of their lack on the ground at La Fossa crater.

An obvious feature of the sublimate assemblage from Mutnovsky is the abundance of cadmium, thallium and iodine-bearing phases. This cannot be explained only by enrichment of gas with Cd, Tl and I: even higher concentrations of the elements were determined at Kudryavy (Taran *et al.*, 1995), but similar phases were not observed (Churakov *et al.*, 2000). We consider that other factors are also gas composition, especially SO_2 and H_2S abundances, and specific discharging conditions, particularly at low temperatures. Thallium and iodine are elements rarely found at volcanoes. Crystals of native thallium were described among the Momotombo sublimates (Quisefit *et al.*, 1989). Small quantities of Tl-Br phases were found at La Fossa crater (Fulignati & Sbrana, 1998), and only minor amounts of Tl were detected chemically in silica tubes (Cheynet *et al.*, 2000). A. Bernard (1985) reported about $\text{NH}_4\text{Pb}(\text{Br},\text{Tl})$ phase in Merapi tubes and $\text{NH}_4\cdot 2\text{As}_2\text{O}_3\cdot\text{I}(\text{Br})$ phase in the Momotombo tube.

On the contrary, halite and sylvite usually are common phases among sublimates. Our investigation has revealed only low to moderate amount of halite in several tubes, and no sylvite. This may be accounted for by the low (less than usual) content of Na and K in gases. The temperature of the hottest fumaroles is slightly above 500°C. It is lower than the temperature interval of halite-sylvite deposition for

most volcanoes (Symonds *et al.*, 1987; Symonds, 1993; Tkachenko *et al.*, 1999, *etc.*). Not only temperature may be a reason of the low content of Na-K in fumarolic gases, but also some internal features of the hydrothermal system of Mutnovsky. For example, all tubes containing halite had been inserted in vents in the southern part of the fumarolic field, all natural incrustations with NaCl were also found there. Tubes from the northern part of the field (only 8 metres apart) have shown low amounts or no NaCl (corresponding condensate analysis A1). Condensate from the southern part of the fumarolic field (the analysis A0) has relatively high Na concentration in spite of lower temperature.

Volcanic gases usually contain a few ppm As (Vicandy & Minoru, 1993), for example up to 25 ppm were detected at La Fossa crater (Signorelli *et al.*, 1998). In spite of high As concentrations, Cheynet *et al.*, (2000) pointed to the absence of crystallized As minerals among the fumarolic incrustations at La Fossa; undetermined As-S and As-S-Cl phases occur only inside the tubes. The likely reason is a lack of appropriate deposition conditions as mentioned above with regard to low-temperature sulphides and halides: deposition of solid As-bearing species occurs only below 250°C. At Mutnovsky, amorphous arsenious sulphur As₂S₃-S and As-S-I phase occur in sampling tubes below 210°C in reducing conditions and are also widespread in nature (highly oxidizing conditions). Minor amounts of a natural As-S-Cl phase were also discovered at Mutnovsky volcano outside the active crater on a low-temperature fumarolic field.

The abundances and sizes of crystals depend on their nucleation conditions (Sunagawa, 1987; Symonds, 1993). Heterogeneous (gas-phase edge) nucleation, connected with relatively low supersaturations, produces normal crystalline precipitates. Few large euhedral crystals at the highest temperature of phase occurrence and numerous small crystals at low temperature are in accordance with the nucleation rate, which increases along with the degree of supersaturation. Homogeneous nucleation in the gas volume occurs when the degree of supersaturation is extremely high; it forms thin aerosol particles mostly blown away with gas flow. We suggest that X-ray amorphous arsenious sulphur is deposited in just such a way. Arsenic concentrations in gases (6-8 ppm), two order of magnitude higher than heavy metals, leads to high degrees of supersaturation. With cooling of the gas, numerous small fragments of the As₂S₃ crystal lattice are formed in its volume. These nanoparticles deposit together with sulphur to form non-crystalline hollow fibres of As₂S₃-S solid solution. Similar structures are known in a technique for growing artificial arsenic sulphides films from vapours derived from molten As₂S₃ (Pecheritsyn *et al.*, 1998).

Conclusion

1. The sublimates at Mutnovsky volcano change from the simple sulphides (pyrite, greenockite) to complex Cd-Pb-Bi and Pb-As-Bi sulphosalts, Pb-As and Bi sulphohalides and Cd, Tl, Pb, Bi halides with decreasing temperature of deposition. The lowest-temperature phases

are As-bearing compounds and native sulphur. The observed sequence of solids indicates volatile transport of elements in the form of simple species. Quantity and sizes of crystals depend on their nucleation conditions. Homogeneous nucleation in the gas and subsequent deposition of fine aerosol particles may be the mechanism of precipitation of X-ray amorphous sulphur.

2. The main (species-forming) elements in sublimates are Na, Fe, Cd, Tl, Pb, Bi, As, S, Se, Te, Cl, Br and I. Several elements enrich the hot ends (T > 400°C) of the tubes without formation of their own phases. Sn, In, Cu, Zn and Mo are present in concentrations within the limits of 0.1-0.5 weight%; Ag, Au (50-75 ppm), Re (6-17 ppm) and Pt (1 ppm) are also detected here. All the elements, which form their own phases or are appreciably enriched in other phases, are transported in the form of gaseous species. Refractory elements Mg, Ca, Sr, Ba, Al, Ti, and Zr are scattered along the whole length of the tubes in small particles of altered rocks derived from conduit walls.

3. The sublimate assemblage from Mutnovsky is abundant in rare and unique As-, Cd-, Tl- and I-bearing sulphosalts, sulphohalides and halides. This may be explained by peculiar gas composition and specific discharging conditions: a combination of low temperatures with low oxygen fugacity. Sulphosalts Cd₄PbBi₁₂(S,Se)₂₃, CdPb₄Bi₆(S,Se)₁₄, Pb₃(As,Bi)₃S₇Cl and complex halide PbTl₃(Cl,Br,I)₅ occur both in the tubes and on the ground, they may be considered as new minerals.

Acknowledgments: We thank A.V Mokhov and A.T. Titov for their researches with the SEM-EDS, A.I. Tsepina for EMPA identification of sulphosalts, V.K. Karandashev for the high-quality ICP-MS and ICP-AES analyses. We are indebted to E.O. Dubinina for isotopic analyses. We also like to thank V.M. Okrugin for permanent support and logistical assistance and G.M. Gavrilenko for assistance during field works. Reviews by Y.A. Taran and R. Moretti were helpful and constructive. This work was partially supported by grants from RFBR # 99-05-64576 and # 03-05-64324.

References

- Bernard, A. (1985), Les mécanismes de condensation des gaz volcaniques (chimie, minéralogie et équilibres des phases condensées majeures et mineures) PhD thesis, Université Libre de Bruxelles, 412 p.
- Bernard, A.A. & Le Guern, F. (1986): Condensation of volatile elements in high-temperature gases of mount St. Helens. *J. Volcanol. Geotherm. Res.*, **28**, 91-105.
- Borodaev, Y.S., Garavelli, A., Kuzmina, O.V., Mozgova, N.N., Organova, N.I., Trubkin, N.V., Vurro, F. (1998): Rare sulfosalts from Vulcano, Aeolian Islands, Italy. I. Se-bearing kirkiite, Pb₁₀(Bi,As)₆(S,Se)₁₉. *Can. Mineral.*, **36**, 1105-1114.
- Cheyne, B., Dall'Aglia, M., Garavelli, A., Grasso, M.F., Vurro, F. (2000): Trace elements from fumaroles at Vulcano Island (Italy): rates of transport and a thermochemical model. *J. Volcanol. Geotherm. Res.*, **95**, 273-283.
- Churakov, S.V., Tkachenko, S.I., Korzhinskii, M.A., Bocharnikov, R.E., Shmulovich, K.I. (2000): Evolution of Composition of

- High-Temperature Fumarolic Gases from Kudryavy Volcano, Iturup, Kuril Islands: the Thermodynamic Modeling. *Geochem. Int.*, **38**, 436-451.
- Fulignati, P. & Sbrana, A. (1998): Presence of native gold and tellurium in the active high-sulfidation hydrothermal system of the La Fossa volcano Vulcano, Italy. *J. Volcanol. Geotherm. Res.*, **86**, 187-198.
- Garavelli, A., Laviano, R., Vurro, F. (1997): Sublimate deposition from hydrothermal fluids at the Fossa crater – Vulcano, Italy. *Eur. J. Mineral.*, **9**, 423-432.
- Le Guern, F. & Bernard, A.A. (1982): New method for sampling and analyzing volcanic sublimates. Application to Merapi volcano. *J. Volcanol. Geotherm. Res.*, **12**, 133-146.
- Mosgova, N.N., Kuzmina, O.V., Organova, N.I., Laputina, I.P. (1985): New data on sulphosalt assemblages at Vulcano (Italy). *Rend. Soc. It. Mineral. Petrol.*, **40**, 277-283.
- Mosgova, N.N., Organova, N.I., Borodaev, Yu.S., Ryabeva, E.G., Sivtsov, A.V., Getmanskaya, T.I., Kuzmina, O.V. (1998): New data on cannizzarite and bursait. *N. Jb. Miner. Abh.*, **158**, 293-309.
- Myravyyev, A.V., Polyak, B.G., Turkov, V.P., Kozlovteva, S.V. (1983): Second estimation of fumarolic heat flow at Mutnovsky volcano (Kamchatka). *Volc. Seis.*, **5**, 51-63 (in Russian).
- Pecheritsyn, I.M., Kryzhanovsky, I.I., Mikhailov M.D. (1998): Optical properties of amorphous As₂S₃ films depending on preparation conditions. *Glass phys. & chem.*, **24**, 721-729 (in Russian).
- Polyak, B.G. (1966): Geothermal features of present volcanism areas on Kamchatka example. Hauka, Moscow, 180 p (in Russian).
- Quisefit, J.P., Toutain, J.P., Bergametti, G., Javoy, M., Cheynet, B., Person, A. (1989): Evolution versus cooling of gaseous volcanic emissions from Momotombo Volcano, Nicaragua: Thermochemical model and observations. *Geochim. Cosmochim. Acta*, **53**, 2591-2608.
- Serafimova, E.K. (1966): Chemical composition of fumarolic gases at Mutnovsky volcano. *Bull. volcanol. Stations*, **42**, 56-65 (in Russian).
- (1979): Mineral parageneses of sublimates and incrustations of Kamchatkan volcanoes. Hauka, Moscow, 167 p (in Russian).
- Selyangin, O.B. (1993): New data on Mutnovsky volcano: structure, evolution, development. *Volc. Seis.*, **1**, 17-35 (in Russian).
- Signorelli, S., Buccanti, A., Martini, M., Piccardi, G. (1998): Arsenic in fumarolic gases of Vulcano (Aeolian Islands, Italy) from 1978 to 1993: Geochemical evidence from multivariate analysis. *Geochem. J.*, **32**, 367-382.
- Sunagawa, I. (1988): Morphology of Crystals. Part B: Fine Particles, Minerals and Snow. Terra Sci Publ. Co., Tokyo, Japan, 391p.
- Symonds, R. (1993): Scanning electron microscope observations of sublimates from Merapi Volcano, Indonesia. *Geochem. J.*, **26**, 337-350.
- Symonds, R.B. & Reed, M.H. (1993): Calculation of multicomponent chemical equilibria in gas-solid-liquid systems: calculation methods, thermochemical data and applications to studies of high-temperature volcanic gases with examples from Mount St. Helens. *Am. J. Sci.*, **293**, 758-864.
- Symonds, R.B., Rose, W.I., Reed, M.H., Lichte, F.E., Finnegan, D.L. (1987): Volatilization, transport and sublimation of metallic and non-metallic elements in high temperature gases at Merapi Volcano, Indonesia. *Geochim. Cosmochim. Acta*, **51**, 2083-2101.
- Symonds, R.B., Reed, M.H., Rose, W.I. (1992): Origin, speciation and fluxes of trace-element gases at Augustine volcano, Alaska: Insights into magma degassing and fumarolic processes. *Geochim. Cosmochim. Acta*, **56**, 633-657.
- Taran, Y.A., Pilipenko, V.P., Rozhkov, A.M., Vakin, E.A. (1992): A geochemical model for fumaroles of the Mutnovsky volcano, Kamchatka, USSR. *J. Volcanol. Geotherm. Res.*, **49**, 269-283.
- Taran, Y.A., Hedenquist, J.W., Korzhinskii, M.A., Tkachenko, S.I., Shmulovich, K.I. (1995): Geochemistry of magmatic gases from Kudryavy Volcano, Iturup, Kuril Islands. *Geochim. Cosmochim. Acta*, **59**, 1749-1761.
- Taran, Y.A., Bernard, A., Gavilanes, J.-S., Lunezheva, D., Cortes, A., Armenita, M.A. (2001): Chemistry and mineralogy of high-temperature gas discharges from Colima volcano, Mexico. Implications for magmatic gas-atmosphere interaction. *J. Volcanol. Geotherm. Res.*, **108**, 245-264.
- Tkachenko, S.I., Porter, R.P., Korzhinskii, M.A., van Bergen, M.J., Shmulovich, K.I., Shteinberg, G.S. (1999): Studying of ore- and mineral-forming processes in high-temperature fumarolic gases at Kudryavy volcano, the island of Iturup, Kuriles. *Geochemistry*, **4**, 410-422 (in Russian).
- Vakin, E.A., Kirsanov, I.T., Pronin, A.A. (1966): Active crater of Mutnovsky volcano. *Bull. Volcanol. Stations*, **40**, 25-36 (in Russian).
- Vakin, E.A., Kirsanov, I.T., Kirsanova, T.P. (1976): Thermal fields and hot springs of the Mutnovsky geothermal area. In "Geothermal systems and thermal fields of Kamchatka", Hauka, Moscow, 85-114 (in Russian).
- Vicandy, S.M. & Minoru, Y. (1993): Behavior of arsenic in volcanic gases. *Geochem. J.*, **27**, 351-359.
- Zelenski, M.E., Ovsyannikov A.A., Gavrilenko G.M., Seniokov S.L. (2002): Eruption of the Mutnovsky volcano, Kamchatka, on March 17, 2000. *Volc. Seis.*, **6**, 25-28 (in Russian).
- Zelenski, M.E. (2003): Transport of elements and mineral forming conditions at high-temperature gas discharges from Mutnovsky volcano (Kamchatka). PhD thesis, Institute of Volcanology, Petropavlovsk-Kamchatsky, 121 p (in Russian).
- Zoller, W.H., Parrington, J.R., Phelan, J.M. (1983): Iridium enrichment in airborne particles from Kilauea volcano, January 1983. *Science*, **222**, 1118-1121.

Received 1 October 2003

Modified version received 20 May 2004

Accepted 4 October 2004